

Structural and Thermoelectric Properties of Bismuth Telluride – Carbon Composites.

Bartosz Trawiński¹, Beata Bochentyn*¹, Natalia Gostkowska¹, Marcin Łapiński¹, Tadeusz Miruszewski¹, Bogusław Kusz¹

¹Gdańsk University of Technology, Faculty of Applied Physics and Mathematics, Department of Solid State Physics, ul. G. Narutowicza 11/12 80-233 Gdańsk, Poland

*Corresponding author: bbochentyn@mif.pg.gda.pl

Abstract

Carbon nanotubes and amorphous carbon have been introduced into a bismuth telluride matrix (0.15 and 0.30 wt. % ratio) to investigate the influence of the carbon on the composite's thermoelectric properties. Composites with well-dispersed additives have been obtained by sonication and ball-milling methodology. Carbon nanotubes and an amorphous carbon addition led to a decrease in electric conductivity from 1120 S/cm to 77 S/cm. The absolute value of the Seebeck coefficient was found to be reduced, changing from $-113 \mu\text{V/K}$ to $+2 \mu\text{V/K}$, this is attributed to electron trapping by an amorphous carbon. For all investigated composites the phonon contribution of the thermal conductivity increased in comparison with a specimen without carbon additives.

Keywords: thermoelectric materials, composites, carbon nanotubes, amorphous carbon, bismuth telluride

1. Introduction

Thermoelectric materials are recently being investigated and developed with the aim of increasing

their efficiency and therefore their applicability. Nanostructuring of the material provides the most promising possibilities in this area. Low-dimensional materials are observed to have enhanced thermoelectric properties in comparison to bulk materials [1]. These expectations have been experimentally confirmed [2, 3]. However, manufacturing of low dimensional materials is complicated and is not efficiently scalable. Therefore, bulk materials containing nanoinclusions can provide solutions which are more attainable [1, 4]. These structures can be either intrinsic (nanoparticles of matrix material) or extrinsic (different phases introduced to the matrix). The most important impact of nanoinclusions on the materials' properties is that they can decrease the lattice thermal conductivity by scattering of phonons, due to the introduction of defects and/or grain boundaries.

Komentarz [A1]: This sentence is not needed, add the references to the previous sentence.

Varying carbon species have been utilized as additives in thermoelectric nanocomposites. Fullerenes, C_{60} , have been used in conjunction with bismuth telluride based matrixes [4 - 9] , and $CoSb_3$ based materials [10, 11], Si-Ge compounds [12], and Ni-Mo-Sb-Te phases [13]. In most cases, a milling procedure was successfully used for mixing the matrix material with fullerenes. It was also noted that the addition of carbon to Si and Ge substrates, before mechanical alloying, leads to a destruction of the C_{60} structures and gives rise to SiC phase formation [12]. In the case of the Ba-filled $CoSb_3$, skutterudite mixing with fullerenes led to a formation of barium fulleride [11]. The fullerene barrier at grain boundaries prevents recrystallization and grain growth during thermal treatment [6]. Overall, the investigations show [4-6, 8, 10, 11, 13] that the addition of fullerenes results in a decrease of thermal conductivity due to phonon scattering.

Previous work has shown that C_{60} fullerene act as a n-type dopant, leading to a decrease in the carrier concentration in p-type materials [4, 12]. However, the authors of a paper [4] have also shown, that for long composite mixing times, the inverse relationship in the carrier concentration is possible and there is a strong dependence on the temperature. Moreover, further research [6]



revealed that fullerenes are electron acceptors. Measurements of the Hall effect [4, 12] show decreased values of the carrier mobility for materials with fullerenes, resulting in an overall decreased electrical conductivity. This can compensate for changes in a lattice thermal conductivity or even lead to a lower thermoelectric figure of merit (zT) for composites, when compared to the pure matrix materials [6, 13]. In one study, [8] 0.25% (by volume) of fullerenes gave higher electrical conductivity. Cook *et al.* [12] observed that the size of the inclusions should be fitted to the wavelength of the phonons transporting a major part of the thermal energy.

Carbon nanotubes (CNTs) have been investigated as possible additives into thermoelectric materials. CNTs are added to decrease the thermal conductivity by phonon scattering. Unfortunately, the addition of nanotubes also affects the transport of charge carriers by the same mechanism. There are several difficulties with introducing CNTs into crystalline materials with an appropriate dispersion, therefore they are more often used with organic thermoelectric materials [14]. However, procedures based on ultrasonic [15, 16] or mechanical (grinding, milling) [17 - 24] mixing can lead to a well-dispersed composite. Another method is to precipitate the matrix material from solution, in which nanotubes are suspended. This procedure has been used by Kim *et al.* for creating functionalized CNTs [14, 25].

CNTs present a positive value of the Seebeck coefficient (about $20 \mu\text{V/K}$) [15]. Therefore, they can potentially increase the Seebeck coefficient of a composite [15, 20]. However, in p-type materials this value can be decreased because of the reduced value of CNTs thermopower [18]. Khasimsaheb *et al.* [22] considered other mechanisms for influencing the thermoelectric properties, including changes in the electrical conductivity (by affecting mobility) or the energy filtering effect. A principle of this effect is blocking of the low-energy carriers at introduced energy barriers. Only the high energy carriers can diffuse over the energy barrier, which results in a higher thermoelectric voltage, and therefore a higher Seebeck coefficient. The height of the barrier should be around 1-10



times of the kT thermal energy [1]. Tang *et al.* [16] has reported, that the influence of a carbon additive on the properties of a composite has a temperature dependence.

A decreased electrical conductivity due to a reduced mobility is reported in most of publications covering nanotube composites. Other research [14] has shown an increased carrier mobility. In that specific study, it was compensated by a lower concentration of carriers in an n-type Bi_2Te_3 .

A high concentration of CNTs leads to their percolation and the formation of a well-conducting network [26]. It is expected [15, 18], that the introduction of 1D nanostructures into the thermoelectric matrix can cause an increase in its electrical conductivity rather than in its thermal conductivity. However, experimental data presented [21] for Bi_2Te_3 containing 5% CNTs, shows a higher thermal conductivity, compared to pure samples, which is correlated with a decreased electrical conductivity. The presence of highly conducting areas was also observed in composites containing bismuth telluride (or bismuth antimony telluride) and graphene [27, 28]. The addition of 2D carbon resulted in the carrier mobility being enhanced, which is correlated with their concentration. This effect has also been correlated with a higher thermal conductivity in graphene containing samples. For a small amount of carbon, opposite changes in electrical and thermal conductivity have been observed. Interestingly, composites of $(\text{Bi,Sb})_2\text{Te}_3$ with CNTs, [23] had an increased total thermal conductivity and its lattice part, when compared with a pure material. This has been correlated with a decreased electrical conductivity.

In some publications it is stated that an impact of low dimension carbon species on electrical properties, is also based on a simultaneous introduction of defects into the crystal structures [16, 17, 21, 28] or modifications of the electron band structure [9]. Another important role of nanostructured additives, especially CNTs [29], is the reinforcement of the matrix material, extending its fracture strength and its thermal shock resistance.

Komentarz [A2]: Does the author mean low dimensional? Or 1D?



In the case of a bismuth telluride mixed with CNTs, a small (eg. 0.12% wt [20]) amount of additive is the best to optimize the thermoelectric figure of merit (zT). In the presented study, the influence of carbon nanotubes on the thermoelectric properties of bismuth telluride is investigated. These composites are compared with materials containing amorphous carbon (a-C), instead of CNTs. Due to this modification it will be possible to understand whether the low dimensionality of the used additives plays a significant role. If the addition of both forms of carbon results in similar composite properties, CNTs can be replaced by a-C which is cheaper and easier to process. The influence of carbon remaining after poly(vinyl alcohol) (PVA) pyrolysis is also investigated.

2. Materials and methods

Bismuth telluride powder was prepared by an oxide reduction procedure. This method has been previously reported [30-34] as an easy, cheap and effective way to obtain thermoelectric compounds such as Bi-Te [30,31], Bi-Sb-Te [31,32], Te-Ag-Ge-Sb [33] or Cs-Bi-Te [34]. The bismuth and tellurium oxides (Alfa Aesar, 99.99%) were mixed in an appropriate ratio, and ball-milled for 10 hours at 300 rpm speed. The milling procedure was conducted in ZrO_2 bowls, with ZrO_2 balls in an isopropanol environment. The powder was then sintered in a hydrogen atmosphere for 1 hour at 400 °C. It was then ground and pressed at uniaxial pressure of 700 MPa. Pellets were sintered for 10 hours in the same conditions and subsequently ground.

To mix the different species of carbon with Bi_2Te_3 powders, several suspensions were prepared. Two different compositions for each carbon form were used. An amorphous carbon (particle size 50-120 nm) and CNTs (6-9 nm diameter, 5 μ m length) were weighted to make samples containing 0.15 % and 0.30 % carbon by weight. The samples are denoted as BT:AC0.15, BT:AC0.30 (amorphous carbon), BT:CNT0.15 and BT:CNT0.30 (CNT). The carbon was put into beaker,

together with a solution of liquid soap (Ludwik, Inco S.A., Poland). The volume of soap was 2.7 μl per 1 mg of carbon. The suspension was prepared with approximately 5 ml of deionized water, in an ultrasonic bath, with heating up to 70 °C in order to decrease the amount of water. It should be noted here, that during the sonication process it is easier to make a well-dispersed suspension from an amorphous carbon than from nanotubes. It is also a more stable procedure. The suspension was poured into the ball milling bowls, with an appropriate amount of bismuth telluride powder, and ground with ZrO_2 balls for 10 hours at 300 rpm. A paste-like product was then dried and pressed into pellets under 700 MPa pressure. The samples were finally sintered in hydrogen for 20 hours at 400 °C.

A reference sample without any carbon was prepared without the sonication stage (denoted as BT). The same procedure, without sonication, was used to prepare samples with soap, denoted as BT:SOAP and with PVA (BT:PVA). The sample with soap (concentration of which was corresponding to the 0.30% a-C/CNT samples and can be estimated at less than 0.1 wt. %) was prepared in order to determine the surfactants impact on the final composite. The concentration of PVA was chosen to obtain 0.30 wt. % of the elemental carbon from carbonized PVA in a final composite.

To investigate the microstructure of composites and the dispersion of the carbon additives a scanning electron microscopy (SEM) analysis was performed using a FEI Quanta FEG 250 microscope with a secondary electron detector. Powder X-ray powder diffraction (pXRD) analysis (with the Philips X'Pert Pro MPD diffractometer using $\text{CuK}\alpha$ radiation) was used to determine the phase composition and the crystal structure of materials. X-ray photoelectrons spectroscopy (XPS) was utilized to investigate the structure of the carbon in the investigated composites. To remove natural carbon contamination from the surface (from atmosphere), the samples were etched with Ar ions before the XPS measurement. The XPS analysis was carried out with a Omicron



NanoTechnology Argus X-ray photoelectron spectrometer, while the photoelectrons were excited using MgK α radiation.

The electrical conductivity was measured between a 30 °C to 150 °C temperature range using a conventional DC four-probe method, with 5 % uncertainty. The Seebeck coefficient was measured against copper over the same temperature range, with 10 % uncertainty. Archimedes' method was used to determine the density of samples.

The thermal conductivity of samples was determined at 30 °C using home-made equipment. The uncertainty of this measurement was estimated to equal 15 %. The operation of the equipment is based on the measurement of the heat transfer under vacuum conditions between the copper blocks, which were connected to the measured sample.

3. Results and discussion

The SEM images of the investigated materials and the applied carbon additives are presented in Fig 1. The SEM image of pure bismuth telluride (Fig. 1a.) shows a typical result for this materials microstructure with flattened grains and visible parallel edges, indicating a layered crystal structure of Bi₂Te₃. The BT:PVA (Fig. 1b.) sample differs from the pure material. In these samples small, irregularly shaped particles, some of which are marked with circles in Fig. 1b, are observed. Based on this difference, it can be assumed, that these particles are residues of the PVA pyrolysis. Similar particles are visible in the SEM image of the BT:SOAP sample (Fig. 1c).

The SEM image of the BT:CNT0.30 sample (Fig. 1d.) (also representative of the BT:CNT0.15 sample) shows single nanotubes, marked with arrows, distributed between the crystalline grains. A comparison with micrographs of pure CNTs (Fig. 1e.) shows that only the CNTs with the largest radii are visible in the composite. The possible explanation for this is that the smaller nanotubes are



too small to be visible against the background of the Bi_2Te_3 grains. Another possible explanation is that during the sintering process the carbon nanotubes were embedded inside the matrix of grains, like has been previously reported for alumina composites [35].

The composites prepared with amorphous carbon (Fig. 1f. for 0.30% content of a-C) also contain small particles, like for the BT:SOAP sample, to which only soap was introduced. However, these particles have a size like particles from the amorphous carbon, presented in the inset of Fig. 1f. Moreover, the amorphous carbon tends to form films on the grain boundaries, which may be undetectable by SEM imaging. Therefore, the exact origin of the particles in the samples containing amorphous carbon cannot be determined.

The SEM micrographs presented in Fig. 1. shows several pores in the analyzed samples, what is consistent is the small relative density of the samples (presented in Table 1.), which varies between 81 and 89 % of the theoretical value (7.85 g/cm^3).

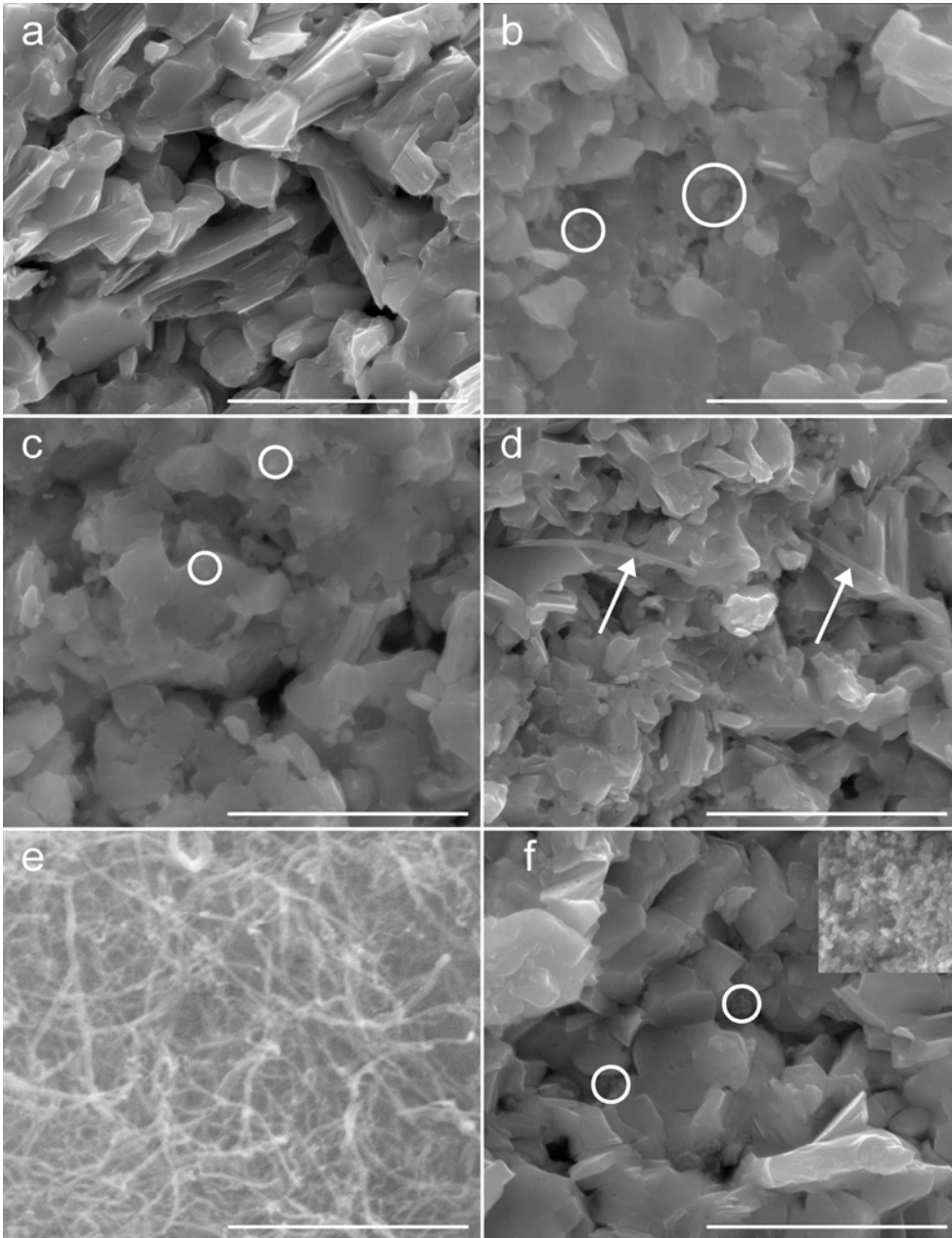
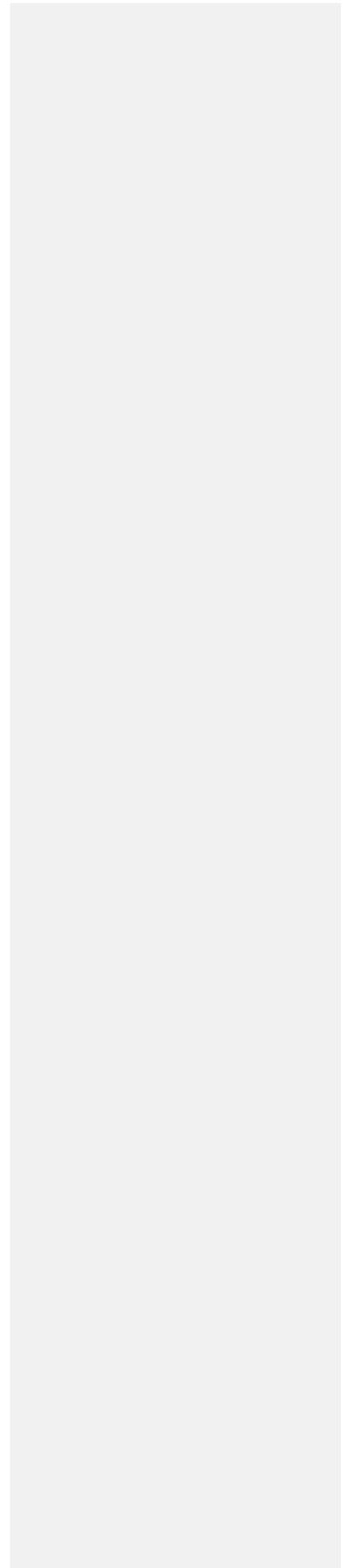


Fig. 1. The SEM images of a) pure bismuth telluride, BT; b) the composite BT:PVA; c) the reference sample with soap only, BT:SOAP; d) the composite with CNT, BT:CNT0.30; e) the carbon nanotubes; f) the composite with amorphous carbon, BT:AC0.30. Inset: the amorphous carbon (identical scale). The white scale bars are 3 μm . The circles highlight the particles of a-c,



the arrows show the CNTs.

The crystal structure of sample was analyzed by pXRD method. The XRD patterns are presented in Fig. 2. As observed, all the reflections match those of Bi_2Te_3 in a crystalline phase, in all investigated materials.

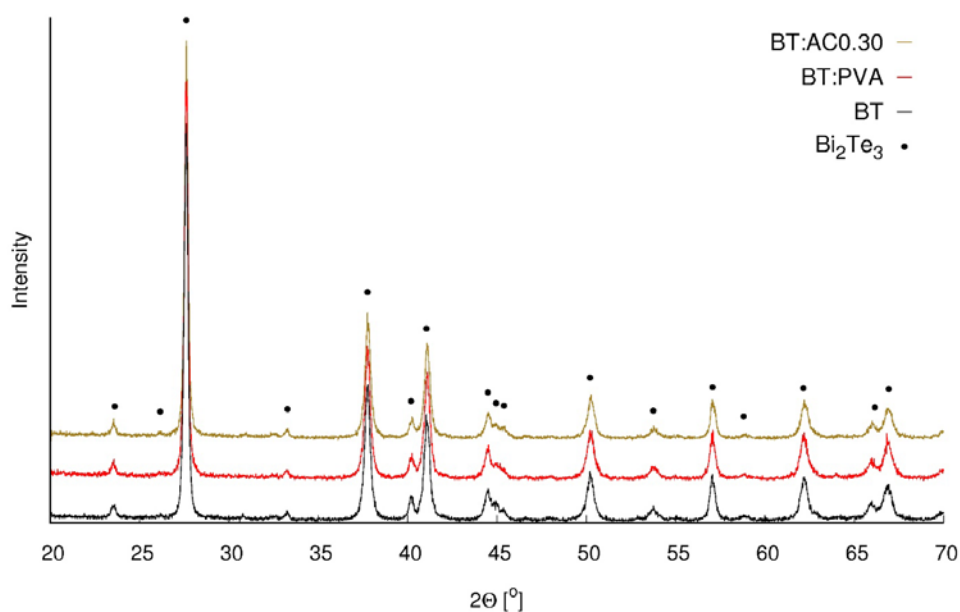


Fig. 2. The XRD patterns of a selection of the samples. The vertical displacement of the patterns is for clarity only.

The XPS measurements were performed on the BT, BT:CNT0.30 and BT:AC0.30 samples. The XPS spectra of the C1s region are presented in Fig. 3. The C1s spectra were deconvoluted to several characteristic peaks. The peak at 284.5 eV is correlated with the sp^2 bonds groups, the binding energy difference between sp^2 and sp^3 is 1.3 eV for carbon nanotubes [36]. The additional peaks correspond to C-O, C=O and C-OOH groups at approximately 286.2 eV, 287.5 eV and 288.7 eV, respectively [36-38]. The deconvoluted spectrum of the BT sample, with C-C, C-O and a small number of C-OOH peaks is characteristic for a natural carbon contamination. It is well documented

that carbon nanotubes have mainly sp² hybridization [39]. From the deconvoluted spectrum of the BT:CNT0.30 sample, sp² to sp³ ratio is calculated to be 4:1. It confirms a presence of carbon nanotubes. The small amount of sp³ hybridized carbon may suggest a defected structure of CNTs. For the BT:AC0.30 sample, the sp² to sp³ ratio is equal 1:1.1. It suggests the presence of amorphous carbon in the sample. The carbon-oxygen groups detected in both BT:CNT0.30 and BT:AC0.30 samples can be interpreted as a result of the addition of soap and of the functionalization of the CNTs.

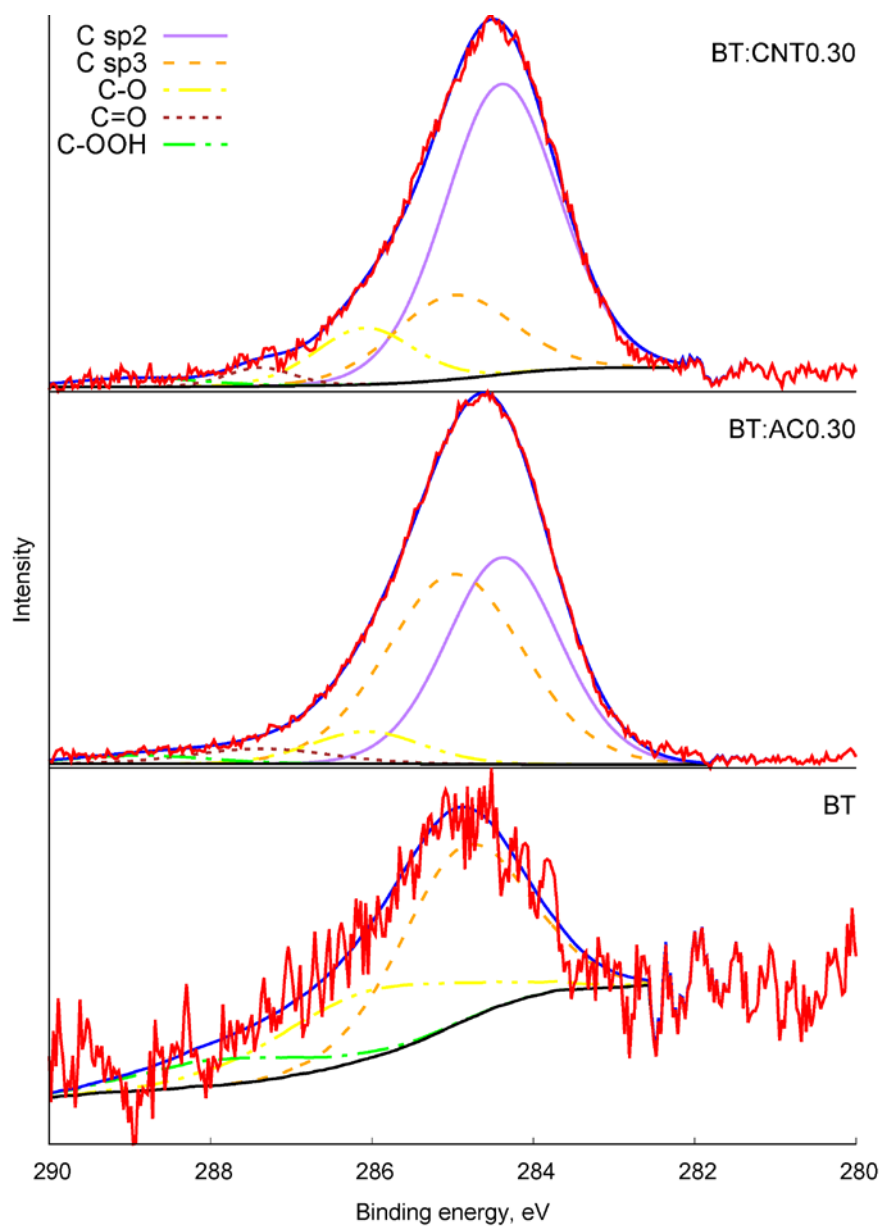


Fig. 3. The XPS spectra of C1s region.

The electrical conductivity of composites was measured between a 30 to 150 °C temperature range. The obtained results are presented in Fig. 4. The values of electrical conductivity noted at 30°C, are denoted in Table 1 together with the other thermoelectric properties at this temperature. The

measured values measured for Bi_2Te_3 are typical for this material [7, 40]. For all the investigated composites with Bi_2Te_3 and varying carbon species, the conductivity is lower than that of a pure bismuth telluride specimen. When compared to the BT:SOAP sample, the BT:CNT0.15 composite has a quite similar electrical conductivity. The samples with nanotubes present higher electrical conductivity than those with a similar concentration of amorphous carbon. This can be assigned to a high conductivity of the CNTs, which provide pathways for easier charge carrier transport. The concentrations of 0.15 and 0.30 %, by weight, correspond to a significantly higher volume fractions of 0.6% and 1.2 %, respectively and a-C; 0.9% and 1.7% for CNTs. In the case of the nanotubes, the scattering exceeds the positive influence of their high electrical conductivity, as observed in previous studies [15, 22]. For the BT:PVA sample, changes in the conductivity are lower than in the case of the BT:AC materials. This is due to a differing introduction technique, meaning the a-C has a different distribution. After the milling stage, the PVA could also form crystals instead of forming films on grain boundaries. A thermal treatment temperature (400°C) is enough to carbonize PVA [41].

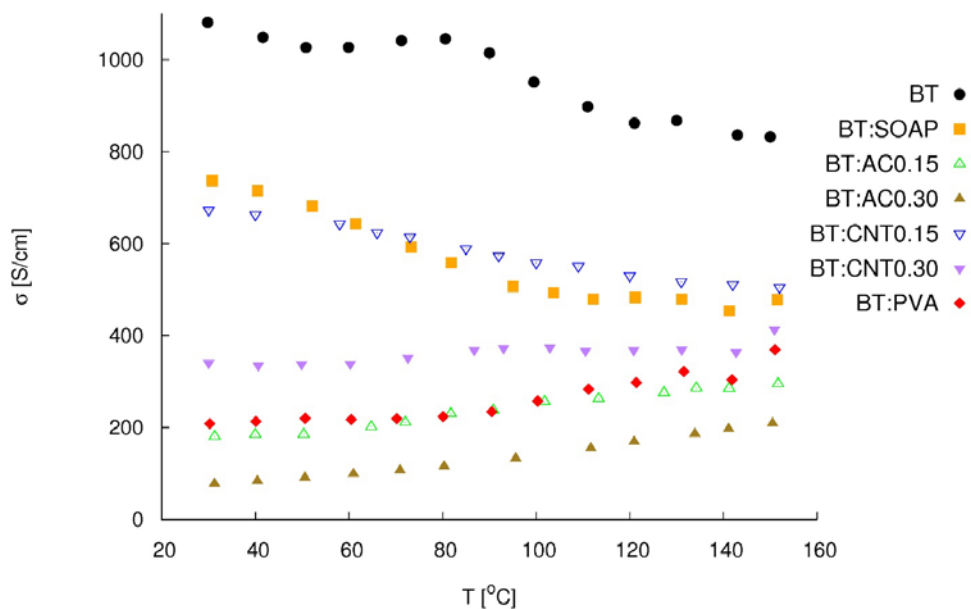


Fig. 4. The temperature dependence of the electrical conductivity of the investigated materials.

In case of samples with amorphous carbon and high concentration of CNTs, the increase of electrical conductivity with temperature was noted. This suggests that the activation mechanism exceeds the transport of the carriers.

Table 1. The properties of the investigated materials at 30 °C.

Sample	Relative density	Seebeck coefficient, $\mu\text{V/K}$	Electrical conductivity, S/cm	Thermal conductivity, W/mK			Figure of Merit (ZT)
				total	electron	phonon	
BT	0.85	-113	1080	1.3	0.52	0.78	0.32
BT:SOAP	0.83	-113	740	1.2	0.36	0.84	0.24
BT:AC0.15	0.86	-85	180	1.0	0.09	0.91	0.04
BT:AC0.30	0.81	-29	77	0.9	0.04	0.86	0.002

BT:PVA	0.89	+1,7	210	1.0	0.10	0.90	0.00002
BT:CNT0.15	0.81	-115	670	1.1	0.33	0.77	0.25
BT:CNT0.30	0.86	-163	340	1.2	0.17	1.03	0.23

The Seebeck coefficient values of the investigated composites were measured over the same temperature range as the electrical conductivity (Fig. 5). A pure bismuth telluride has a negative thermopower, as expected for a n-type material. The addition of amorphous carbon resulted in a decrease of the absolute value of the Seebeck coefficient. For the BT:PVA sample, the thermopower reaches low positive values at temperatures below 50 °C. The influence of holes on the thermoelectric effects becomes stronger, than the influence of the composite's electrons. With increasing temperatures, this effect gradually disappears. This can be explained by the activation of electrons, which is consistent with an increasing electrical conductivity. Taking into consideration a significantly lower conductivity of samples with amorphous carbon, it is observed that a-C is a strong electron acceptor and quenches these carriers in the composite. The high concentration of carbon nanotubes resulted in a higher absolute value of the Seebeck coefficient in the low temperature region. This is unexpected for CNTs, which have a positive thermopower. Kim *et al.* reported that Bi₂Te₃ composites with functionalized nanotubes [14, 25] have an absolute value of the Seebeck coefficient which is increased after CNTs addition. This is consistent with a defected structure of nanotubes, as shown in the XPS results. In other literature reports [14, 25], changes in the Seebeck coefficient were correlated with a decreased concentration of the charge carriers.

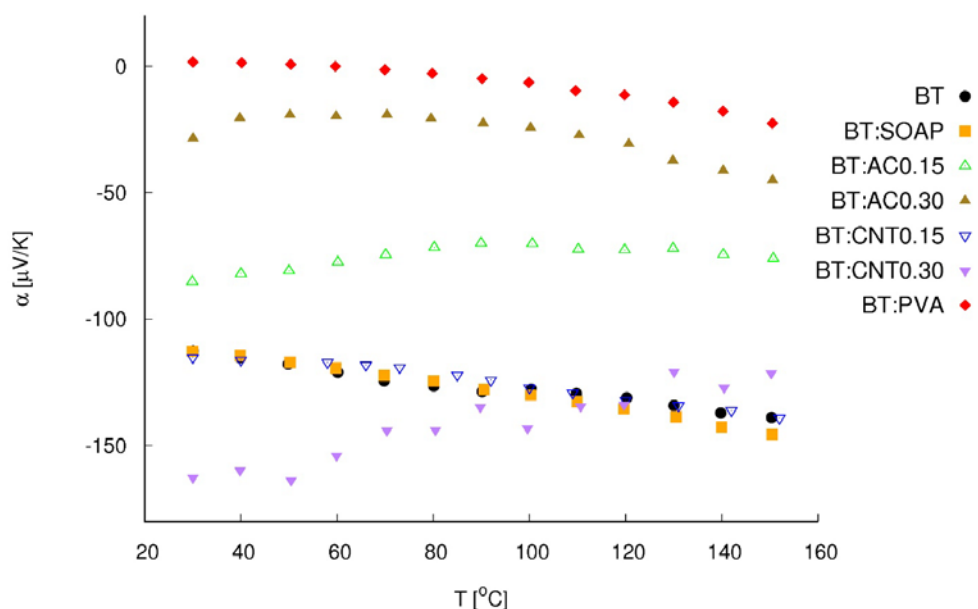


Fig. 5. The temperature dependence of the Seebeck coefficient of the investigated materials.

The thermal conductivity was measured at an ambient temperature of 30 °C. The results are given in Table 1. The electron part of the thermal conductivity was calculated using the Wiedemann-Franz equation ($\kappa = L\sigma T$). The Lorenz number L was assumed to equal $1,6 \cdot 10^{-8} \text{ W}\Omega\text{K}^{-2}$ [23]. The phonon part is the difference between the total and the electron part. The calculated phonon part of the thermal conductivity was higher in materials with carbon additives. Similarly, unexpected result have previously been obtained for composites containing bismuth telluride and carbon nanotubes [23]. This can be explained by a high thermal conductivity of CNTs, about 15 W/mK, mainly a phonon contribution [42]. Therefore, in a porous structure, the thermal bridges formed by the CNTs can enhance the phonon thermal conductivity. This does not explain the increased phonon part of thermal conductivity in the composites with an amorphous carbon. However, in all samples, the value is equal in terms when considering the uncertainty of the measurements.

Komentarz [A3]: Check this...



Finally, the thermoelectric figure of merit was calculated. The investigated composites had lower ZT, than a pure bismuth telluride, owing to the low Seebeck coefficient (especially in the BT:PVA case) and electrical conductivity (especially in the BT:AC0.30 composite).

4. Conclusions

The well-dispersed composites of bismuth telluride and varying forms of carbon were prepared via both sonication and ball-milling procedures. The carbon nanotubes and amorphous carbon were utilized as additives in a 0.15 and 0.30 wt.% ratio. Soap was used to improve the dispersion of carbon. A comparable sample with only soap was investigated to determine its influence on the composites' properties. It was found that the addition of soap has a strong negative influence on the thermoelectric properties of the analyzed composites. Additionally, the sample with carbon obtained from poly(vinyl alcohol) carbonization was investigated.

Komentarz [A4]: What does this show?

The observed changes of the material's properties with the carbon addition are motivating. Typically, the Seebeck coefficient increase is correlated with a lower conductivity, and a lower thermopower with higher conductivity [14, 19, 20, 22, 29]. In another publications, the observed changes in the electrical conductivity are usually smaller. In this study, amorphous carbon was found to be acting as an electron acceptor, trapping conduction band electrons, decreasing both electrical conductivity and an absolute value of the Seebeck coefficient (even up to a positive value). For a sample with a pyrolyzed PVA, the observed changes of the electrical conductivity were smaller and the changes of the Seebeck coefficient are higher than in materials with amorphous carbon. This effect suggests, that the amorphous carbon can have an improved impact on p-type materials. Further research may provide better understanding of the a-C influence on the properties of these thermoelectric materials.



The observed decrease in electrical conductivity suggests that lower concentrations of carbon should be used in further research. The composites with carbon nanotubes had higher electrical conductivity than those with a-C, this is a consequence of their high conductivity and formation of long bridges for charge carrier transport. This positive influence was compensated by scattering. Therefore, in terms of nanotubes, the lower concentrations should be used. The sample with 0.3% of CNTs had higher Seebeck coefficients, similarly to previous results for composites with functionalized nanotubes. This is consistent with the XPS results, which revealed a defected structure of nanotubes, containing contaminant oxygen groups.

Unexpectedly, the carbon containing composites had a higher phonon part of the thermal conductivity. This, together with the lower electrical conductivity and the Seebeck coefficient resulted in a significantly decreased thermoelectric figure of merit.

Funding

This work was supported by the National Science Center under the grant No. NCN 2016/21/B/ST8/03193.

Acknowledgments

The authors would like to acknowledge Dr. Jakub Karczewski for the SEM investigations and Dr. Kamila Żelechowska for help with introducing carbon nanotubes.

References

1. Marisol Martín-González, O. Caballero-Calero, P. Díaz-Chao, Nanoengineering thermoelectrics for 21st century: Energy harvesting and other trends in the field, *Renew. Sust. Energ. Rev.*, Vol. 24, 2013, p. 288-305, doi: 10.1016/j.rser.2013.03.008.
2. Anas I. Abutaha, S. R. Sarath Kumar, Kun Li, Arash M. Dehkordi, Terry M. Tritt, Husam N. Alshareef, Enhanced Thermoelectric Figure-of-Merit in Thermally Robust, Nanostructured Superlattices Based on SrTiO₃, *Chem. Mater.*, Vol. 27, Issue 6, 2015, p. 2165–2171, doi:10.1021/acs.chemmater.5b00144.
3. Genqiang Zhang, Benjamin Kirk, Luis A. Jauregui, Haoran Yang, Xianfan Xu, Yong P. Chen, Yue Wu, Rational Synthesis of Ultrathin n-Type Bi₂Te₃ Nanowires with Enhanced Thermoelectric Properties, *Nano Lett.*, Vol. 12, Issue 1, 2012, p. 56-60, doi:10.1021/nl202935k.
4. N. W. Gothard, T. M. Tritt, J. E. Spowart, *J. Appl. Phys.*, Vol. 110, Issue 2, 2011, 023706, doi:10.1063/1.3606547.
5. N. Gothard, J. E. Spowart, T. M. Tritt, Thermal conductivity reduction in fullerene-enriched p-type bismuth telluride composites, *Phys. Status Solidi*, Vol. 207, Issue 1, 2010, p. 157-162, doi:10.1002/pssa.200925145.
6. V. A. Kulbachinskii, V. G. Kytin, M.Yu. Popov, S. G. Buga, P. B. Stepanov, V. D. Blank, Composites of Bi_{2-x}Sb_xTe₃ nanocrystals and fullerene molecules for thermoelectricity, *J. Solid State Chem.*, Vol. 193, 2012, 64-70, doi:10.1016/j.jssc.2012.03.065.
7. N. Gothard, G. Wilks, T. M. Tritt, J. E. Spowart, Effect of Processing Route on the Microstructure and Thermoelectric Properties of Bismuth Telluride-Based Alloys, *J. Electron. Mater.*, Vol. 39, Issue 9, 2010, p. 1909, 1913, doi:10.1007/s11664-009-1051-5.
8. V. D. Blank, S. G. Buga, V. A. Kulbachinskii, V. G. Kytin, V. V. Medvedev, M. Yu. Popov, P. B. Stepanov, V. F. Skok, Thermoelectric properties of Bi_{0.5}Sb_{1.5}Te₃/C₆₀ nanocomposites, *Phys. Rev. B*, Vol. 86, Issue 7, 2012, 075426, doi:10.1103/PhysRevB.86.075426.
9. Zhou Wang, Aravindkumar Vemishetti, John Idoko Ejembi, Guodong Wei, Boliang Zhang, Li Wang, Li Wang, Yi Zhang, Shengmin Guo, Jia Luo, Corin Chepko, Qilin Dai, Jin Ke, Tang,



- Guang-Lin Zha., High thermoelectric performance of fullerene doped $\text{Bi}_{0.5}\text{Sb}_{1.5}\text{Te}_3$ alloys, *Mater. Sci. Eng. B*, Vol. 205, 2016, p. 36-39, doi:10.1016/j.mseb.2015.12.001.
10. X. Shi, L. Chen, J. Yang, G. P. Meisner, Enhanced thermoelectric figure of merit of CoSb_3 via large-defect scattering, *Appl. Phys. Lett.*, Vol. 84, Issue 13, 2004, p. 2301-2303, doi:10.1063/1.1687997.
11. X. Shi, L. D. Chen, S. Q. Bai, X. Y. Huang, X. Y. Zhao, Q. Yao, C. Uher, Influence of fullerene dispersion on high temperature thermoelectric properties of $\text{Ba}_y\text{Co}_4\text{Sb}_{12}$ -based composites, *J. Appl. Phys.*, Vol. 110, Issue 2, 103709, doi:10.1063/1.2811936.
12. B. A. Cook, J. L. Haringa, S. Loughin, Fullerite additions as a phonon scattering mechanism in p-type Si-20 at.% Ge, *Mater. Sci. Eng. B*, Vol. 41, Issue 2, 1996, p. 280-288, doi:10.1016/S0921-5107(96)01665-0.
13. Nagaraj Nandihalli, Ali Lahwal, Daniel Thompson, Tim C. Holgate, Terry M. Tritt, Véronique Dassylva-Raymond, László I. Kiss, Elisabeth Sellier, Stéphane Gorsse, Holger Kleinke, Thermoelectric properties of composites made of $\text{Ni}_{0.05}\text{Mo}_3\text{Sb}_{5.4}\text{Te}_{1.6}$ and fullerene, *J. Solid State Chem.*, Vol. 203, 2013, p. 25-30, doi:10.1016/j.jssc.2013.03.061.
14. Kyung Tae Kim, Si Young Choi, Eun Hye Shin, Kyong Seok Moon, Hye Young Koo, Gil-Geun Lee, Gook Hyun Ha, The influence of CNT on the thermoelectric properties of a CNT/ Bi_2Te_3 composite, *Carbon*, Vol. 52, 2013, p. 541-549, doi:10.1016/j.carbon.2012.10.008.
15. Hyunwoo Bark, Jin-Sang Kim, Heesuk Kim, Ju-Hyuk Yim, Hyunjung Lee, Effect of multiwalled carbon nanotubes on the thermoelectric properties of a bismuth telluride matrix, *Curr. Appl. Phys.*, Vol. 13, 2013, p. S111-S114, doi:10.1016/j.cap.2013.01.019.
16. Guodong Tang, Wenchao Yang, Jianfeng Wen, Zhuangchun Wu, Cang Fan, Zhihe Wang, Ultralow thermal conductivity and thermoelectric properties of carbon nanotubes doped $\text{Ca}_3\text{Co}_4\text{O}_{9+\delta}$, *Ceram. Int.*, Vol. 41, Issue 1, Part B, 2015, p. 961-965, doi:10.1016/j.ceramint.2014.09.015.
17. Quentin Lognoné, Franck Gascoin, On the effect of carbon nanotubes on the thermoelectric



- properties of n-Bi₂Te_{2.4}Se_{0.6} made by mechanical alloying, *J. Alloy. Compd.*, Vol. 635, 2015, p. 107–111, doi:10.1016/j.jallcom.2015.02.055.
18. Nagaraj Nandihalli, Stéphane Gorsse, Holger Kleinke, Effects of additions of carbon nanotubes on the thermoelectric properties of Ni_{0.05}Mo₃Sb_{5.4}Te_{1.6}, *J. Solid State Chem.*, Vol. 226, 2015, p. 164–169, doi:10.1016/j.jssc.2015.02.016.
19. Dong-Hyun Park, Min-Young Kim, Tae-Sung Oh, Thermoelectric energy-conversion characteristics of n-type Bi₂(Te,Se)₃ nanocomposites processed with carbon nanotube dispersion, *Curr. Appl. Phys.*, Vol. 11, Issue 4, Supplement, International Conference on Electronic Materials and Nanotechnology for Green Environment, 2011, p. S41-S45, doi:10.1016/j.cap.2011.07.007.
20. Y.H. Yeo, T.S. Oh, Thermoelectric properties of p-type (Bi,Sb)₂Te₃ nanocomposites dispersed with multiwall carbon nanotubes, *Mater. Res. Bull.*, Vol. 58, Proceedings of the IFFM2013 - Vol. 1: Fundamentals of the functional materials, 2014, p. 54–58, doi:10.1016/j.materresbull.2014.04.046.
21. Y. Zhang, X. L. Wang, W. K. Yeoh, R. K. Zheng, C. Zhang, Electrical and thermoelectric properties of single-wall carbon nanotube doped Bi₂Te₃, *Appl. Phys. Lett.*, Vol. 101, Issue 3, 2012, 031909, doi:10.1063/1.4737898.
22. B. Khasimsaheb, Niraj Kumar Singh, Sivaiah Bathula, Bhasker Gahtori, D. Haranath, S. Neeleshwar, The effect of carbon nanotubes (CNT) on thermoelectric properties of lead telluride (PbTe) nanocubes, *Curr. Appl. Phys.*, Vol. 17, Issue 2, 2017, p. 306-313, doi:10.1016/j.cap.2016.05.026.
23. Kaleem Ahmad, Chunlei Wan, Mohammad A. Al-Eshaikh, Effect of Uniform Dispersion of Single-Wall Carbon Nanotubes on the Thermoelectric Properties of BiSbTe-Based Nanocomposites, *J. Electron. Mater.*, Vol. 46, Issue 2, 2017, p.1348-1357, doi:10.1007/s11664-016-5095-z.
24. Yuewen Zhang, Xiaopeng Jia, Hairui Sun, Bing Sun, Binwu Liu, Haiqiang Liu, Lingjiao Kong,



- Hongan Ma, Enhanced thermoelectric performance of nanostructured CNT/BiSbTe bulk composite from rapid pressure-quenching induced multi-scale microstructure, *J. Materiomics*, Vol. 2, Issue 4, 2016, p. 316-323, doi:10.1016/j.jmat.2016.08.002.
25. Kyung Tae Kim, Yeong Seong Eom, Injoon Son, Fabrication Process and Thermoelectric Properties of CNT/Bi₂(Se,Te)₃ Composites, *J. Nanomater.*, Vol. 2015, 2015, 202415, doi:10.1155/2015/202415.
26. Huan Pang, Ying-Ying Piao, Ye-Qiang Tan, Guang-Yu Jiang, Jian-Hua Wang, Zhong-Ming Li, Thermoelectric behaviour of segregated conductive polymer composites with hybrid fillers of carbon nanotube and bismuth telluride, *Mater. Lett.*, Vol. 107, 2013, p. 150–153, doi:10.1016/j.matlet.2013.06.008.
27. Hyun Ju, Jooheon Kim, Preparation and structure dependent thermoelectric properties of nanostructured bulk bismuth telluride with graphene, *J. Alloy. Compd.*, Vol. 664, 2016, p. 639-647, doi:10.1016/j.jallcom.2016.01.002.
28. Cong Li, Xiaoying Qin, Yuanyue Li, Di Li, Jian Zhang, Haifeng Guo, Hongxing Xin, Chunjun Song, Simultaneous increase in conductivity and phonon scattering in a graphene nanosheets/(Bi₂Te₃)_{0.2}(Sb₂Te₃)_{0.8} thermoelectric nanocomposite, *J. Alloy. Compd.*, Vol. 661, 2016, p. 389-395, doi:10.1016/j.jallcom.2015.11.217.
29. Fei Ren, Hsin Wang, Paul A. Menchhofer, James O. Kiggans, Thermoelectric and mechanical properties of multi-walled carbon nanotube doped Bi_{0.4}Sb_{1.6}Te₃ thermoelectric material, *Appl. Phys. Lett.*, Vol. 103, Issue 22, 2013, 221907, doi:10.1063/1.4834700.
30. Beata Bochentyn, Jakub Karczewski, Tadeusz Miruszewski, Bogusław Kusz, Structure and thermoelectric properties of Bi-Te alloys obtained by novel method of oxide substrates reduction, *Journal of Alloys and Compounds*, Vol. 646, 2015, p. 1124-1132, doi:10.1016/j.jallcom.2015.06.127.
31. B. Bochentyn, J. Karczewski, T. Miruszewski, B. Kusz, Novel method of metal - oxide glass composite fabrication for use in thermoelectric devices, *Materials Research Bulletin*, Vol. 76,



- 2016, p. 195-204, doi:10.1016/j.materresbull.2015.12.018.
32. B. Bochentyn, J. Karczewski, T. Miruszewski, B. Kusz, Thermoelectric properties of bismuth-antimony-telluride alloys obtained by reduction of oxide substrates, *Materials Chemistry and Physics*, Vol. 177, 2016, p. 353-359, doi:10.1016/j.matchemphys.2016.04.039.
33. B.Kusz, T.Miruszewski, B.Bochentyn, M.Łapiński, J.Karczewski, Structure and thermoelectric properties of Te/Ag/Ge/Sb (TAGS) materials obtained by reduction of melted oxide substrates, *Journal of Electronic Materials*, Vol. 45, 2016, p. 1085-1093, doi:10.1007/s11664-015-4251-1.
34. N.Gostkowska, T.Miruszewski, B.Trawiński, B.Bochentyn, B.Kusz, Structure and thermoelectric properties of Cs-Bi-Te alloys fabricated by different routes of reduction of oxide reagents, *Solid State Sciences*, IN PRESS, doi:10.1016/j.solidstatesciences.2017.07.016.
35. Kaleem Ahmad, Wei Pan, Microstructure-toughening relation in alumina based multiwall carbon nanotube ceramic composites, *J. Eur. Ceram. Soc.*, Vol. 35, Issue 2, 2015, p. 663–671, doi:10.1016/j.jeurceramsoc.2014.08.044.
36. L. Stobinski, B. Lesiak, A. Malolepszy, M. Mazurkiewicz, B. Mierzawa, J. Zemek, P. Jiricek, I. Bieloshapka, *J. Electron. Spectr. Rel. Phenom*, Vol. 195, 2014, p. 145-154, doi:10.1016/j.elspec.2014.07.003
37. Kevin A. Wepasnick, Billy A. Smith, Julie L. Bitter, D. Howard Fairbrother, *Anal. Bioanal. Chem*, Vol. 396, Issue 3, 2010, p. 1003-1014, doi:10.1007/s00216-009-3332-5.
38. Xia Liu, Jiaying Li, Xiangxue Wang, Changlun Chen, Xiangke Wang, *J. Nucl. Mater*, Vol. 466, 2015, p. 56-64, doi:10.1016/j.jnucmat.2015.07.027.
39. Ado Jorio, Riichiro Saito, Gene Dresselhaus, Mildred S. Dresselhaus, *Raman Spectroscopy in Graphene Related Systems*, Wiley-VCH Verlag GmbH & Co, 2011, doi: 10.1002/978352763269.
40. Weishu Liu, Kevin C. Lukas, Kenneth McEnaney, Sangyeop Lee, Qian Zhang, Cyril P. Opeil, Gang Chen, Zhifeng Ren, Studies on the Bi₂Te₃-Bi₂Se₃-Bi₂S₃ system for mid-temperature thermoelectric energy conversion, *Energ. Environ. Sci.*, Vol. 6, Issue 2, 2013, p. 552-560,



doi:10.1039/C2EE23549H.

41. Jeffrey W. Gilman, David L. Vander Hart, Takashi Kashiwagi, Thermal Decomposition Chemistry of Poly(vinyl alcohol), Fire and Polymers II: Materials and Tests for Hazard Prevention, ACS Sym. Ser., 599, 1995, p. 161-185.
42. Da Jiang Yang, Qing Zhang, George Chen, S. F. Yoon, J. Ahn, S. G. Wang, Q. Zhou, Q. Wang, J. Q. Li, Thermal conductivity of multiwalled carbon nanotubes, Phys. Rev. B, Vol. 66, Issue 16, 2002, 165440, doi:10.1103/PhysRevB.66.165440.